PPARδ activation attenuates hepatic steatosis in *Ldlr*$^{-/-}$ mice by enhanced fat oxidation, reduced lipogenesis, and improved insulin sensitivity

Lazar A. Bojic,*,† Dawn E. Telford,*,§ Morgan D. Fullerton, Rebecca J. Ford,** Brian G. Sutherland,* Jane Y. Edwards,*,§ Cynthia G. Sawyez,*,§ Robert Gros,*,†† Bruce E. Kemp,§§ Gregory R. Steinberg,** and Murray W. Huff[1],*,†,§**

Vascular Biology, Robarts Research Institute,* and Departments of Biochemistry,† Physiology and Pharmacology,†† and Medicine,§ The University of Western Ontario, London, Ontario, Canada, N6A 5B7; Division of Endocrinology and Metabolism, Department of Medicine,** McMaster University, Hamilton, Ontario, Canada, L8S 4K1; and St. Vincent's Institute of Medical Research and Department of Medicine,§§ University of Melbourne, Fitzroy, Victoria 3065, Australia

Abstract PPARδ regulates systemic lipid homeostasis and inflammation, but its role in hepatic lipid metabolism remains unclear. Here, we examine whether intervening with a selective PPARδ agonist corrects hepatic steatosis induced by a high-fat, cholesterol-containing (HFHC) diet. *Ldlr*$^{-/-}$ mice were fed a chow or HFHC diet (42% fat, 0.2% cholesterol) for 4 weeks. For an additional 8 weeks, the HFHC group was fed HFHC or HFHC plus GW1516 (3 mg/kg/day). GW1516-intervention significantly attenuated liver TG accumulation by induction of FA β-oxidation and attenuation of FA synthesis. In primary mouse hepatocytes, GW1516 treatment stimulated AMP-activated protein kinase (AMPK) and acetyl-CoA carboxylase (ACC) phosphorylation in WT hepatocytes, but not AMPKβ1$^{-/-}$ hepatocytes. However, FA oxidation was only partially reduced in AMPKβ1$^{-/-}$ hepatocytes, suggesting an AMPK-independent contribution to the GW1516 effect. Similarly, PPARδ-mediated attenuation of FA synthesis was partially due to AMPK activation, as GW1516 reduced lipogenesis in WT hepatocytes but not AMPKβ1$^{-/-}$ hepatocytes. HFHC-fed animals were hyperinsulinemic and exhibited selective hepatic insulin resistance, which contributed to elevated fasting FA synthesis and hyperglycemia. GW1516 intervention normalized fasting hyperinsulinemia and selective hepatic insulin resistance and attenuated fasting FA synthesis and hyperglycemia. The HFHC diet polarized the liver toward a proinflammatory M1 state, which was reversed by GW1516 intervention. Thus, PPARδ agonist treatment inhibits the progression of preestablished hepatic steatosis.—Bojic, L. A., D. E. Telford, M. D. Fullerton, R. J. Ford, B. G. Sutherland, J. Y. Edwards, C. G. Sawyez, R. Gros, B. E. Kemp, G. R. Steinberg, and M. W. Huff. **PPARδ activation attenuates hepatic steatosis in *Ldlr*$^{-/-}$ mice by enhanced fat oxidation, reduced lipogenesis, and improved insulin sensitivity. *J. Lipid Res.* 2014.** 55: **1254–1266.**

Supplementary key words hepatic triglyceride • lipids • adenosine monophosphate-activated protein kinase • insulin resistance • inflammation • energy expenditure

Hepatic steatosis, defined as excessive lipid accumulation in the liver, is observed in >40% of patients with type 2 diabetes (1, 2). Although a causal relationship between hepatic steatosis and insulin resistance has been difficult to define (1), inflammation has been implicated as a contributing factor to dysregulated hepatic insulin signaling (3). As a consequence, hyperinsulinemia-mediated lipogenesis ensues, which along with suppressed FA oxidation contributes to ectopic lipid deposition (4). Prolonged

This work was primarily supported by the Canadian Institutes of Health Research Grant MOP-126045 (M.W.H.); the Heart and Stroke Foundation of Canada Grant PRG-5967 (M.W.H.); and the University of Western Ontario, Department of Medicine Grant POEM (M.W.H.). Additional support was provided by grants from the Canadian Diabetes Association (G.R.S.) and the Canadian Foundation for Innovation (G.R.S., R.G.). Creation of Ampkβ1$^{-/-}$ *mice was supported by grants from the National Health and Medical Research Council (B.E.K., G.R.S.) and the Victorian Government's Operational Infrastructure Support Program (B.E.K.). L. A. Bojic held an Ontario Graduate Scholarship.*

Manuscript received 27 November 2013 and in revised form 24 April 2014.

Published, JLR Papers in Press, May 26, 2014
DOI 10.1194/jlr.M046037

Abbreviations: ACC, acetyl-CoA carboxylase; ACOX, acetyl-CoA oxidase; ADFP, adipocyte differentiation-related protein; ad*PPARD*, adenoviral *PPARD*; Akt, protein kinase B; AMPK, AMP-activated protein kinase; ARG1, arginase 1; β1$^{-/-}$, AMPK β1 subunit knockout; CCL2, chemokine (C-C motif) ligand 2; CCL3, chemokine (C-C motif) ligand 3; CHOP, CCAAT/enhancer binding protein-homologous protein; CPT1a, carnitine palmitoyl transferase 1a; EE, energy expenditure; ER, endoplasmic reticulum; FoXO1, forkhead box protein O1; GRP78, 78 kDa glucose-regulated protein; HFHC, high-fat, cholesterol-containing; ICAM1, intercellular adhesion molecule 1; IL, interleukin; iNOS, inducible NO synthase; INSIG, insulin-induced gene; IRS, insulin receptor substrate; mTORC1, mammalian target of rapamycin complex 1; PCK1, phosphoenolpyruvate carboxykinase 1; PGC1a, PPAR gamma coactivator 1a; RER, respiratory exchange ratio; SREBF, sterol-regulatory element binding factor; SREBP-1c, sterol-regulatory element binding protein 1c; UPR, unfolded protein response.

[1] To whom correspondence should be addressed.
e-mail: mhuff@uwo.ca

hepatic steatosis can result in nonalcoholic steatohepatitis, cirrhosis, and eventually liver failure (3). However, few therapeutic strategies exist that effectively correct hepatic steatosis in the setting of insulin resistance.

At a molecular level, insulin binding to its cognate receptor leads to receptor-mediated tyrosine phosphorylation of insulin receptor substrates (IRS-1 and/or IRS-2), which in turn activate phosphoinositide 3-kinase (PI3-K) to simulate the phosphorylation and activation of protein kinase B (Akt) (5). Normally, insulin-stimulated Akt activation results in the suppression of hepatic gluconeogenesis due to phosphorylation and inactivation of forkhead box (Fox) O1, and the promotion of de novo lipogenesis due to phosphorylation and activation of the mammalian target of rapamycin complex (mTORC) 1 (6). However, in the insulin-resistant liver, Akt loses its ability to inactivate FoxO1 but paradoxically maintains its ability to activate mTORC1 (6). Consequently, mTORC1-driven transcription of the master regulator of lipogenesis, sterol-regulatory element binding protein (SREBP) 1c, remains chronically active (6). In addition, insulin increases the amount of proteolytically processed active SREBP-1c through mechanisms that remain poorly understood (7). In this way, hyperinsulinemia and accompanying hepatic insulin resistance leads to persistent FA synthesis and eventually excessive hepatic lipid accumulation.

In addition to unregulated lipogenesis, decreased fat oxidation exacerbates hepatic lipid accumulation during insulin resistance (8–10). The AMP-activated protein kinase (AMPK) controls cellular and whole-body energy metabolism (11, 12). Specifically, hepatic AMPK is a pivotal regulator of fat oxidation and synthesis, primarily via direct phosphorylation and inhibition of acetyl-CoA carboxylase (ACC) (12–14). Biochemically, this reduces malonyl-CoA levels in the liver, which *i*) depletes FAS of substrate in the lipogenic pathway and *ii*) results in the derepression of carnitine palmitoyl transferase 1a (CPT1a) in the FA oxidation pathway (15). Thus, activation of AMPK provides a potential mechanism for the attenuation of hepatic steatosis.

PPARδ belongs to a class of ligand-dependent transcription factors involved in regulation of glucose and lipid homeostasis (16). A number of animal and human studies have highlighted a potential role for activation of this receptor in the treatment of metabolic disease (17, 18). In mice, genetic manipulations of *Ppard* as well as prevention experiments involving administration of PPARδ agonists revealed that activation of this receptor attenuates dyslipidemia and hyperglycemia, improves whole-body insulin sensitivity, and prevents diet-induced obesity (19–21). However, there are seemingly conflicting and controversial reports with respect to PPARδ activation and hepatic lipid metabolism in mice (19, 22–25). The PPARδ agonist GW1516 attenuated diet-induced hepatic steatosis; however, the 2-fold increase in hepatic acetyl-CoA oxidase (*Acox*) expression suggested a PPARα-dependent effect (22). Tanaka et al. (20) reported that increased expression of genes involved in hepatic fat oxidation resulted in reduced hepatic lipid droplets in high-fat fed mice treated with GW1516. Additionally, in *db/db* mice injected with adenoviral *PPARD* (ad*PPARD*), liver lipid droplets were reduced coincident with decreased SREBP-1c processing, suggesting attenuated lipogenesis (23). Despite reports suggesting reduced hepatic steatosis, other studies have demonstrated that PPARδ activation exerts either no effect (24) or induces liver TG accumulation (19, 25). In *db/db* mice, GW1516 treatment resulted in increased hepatic TG as a result of direct transcriptional activation of acetyl-CoA carboxylase β (*Acc2*), and increased lipogenic gene expression (19). ad*PPARD* gene delivery to high-fat fed $Ldlr^{-/-}$ mice increased both hepatic lipogenic gene expression and hepatic TG accumulation (25). None of these studies actually measured hepatic FA oxidation or synthesis.

The claim that PPARδ activation increases hepatic steatosis is counterintuitive because PPARδ agonists are known to improve whole-body insulin sensitivity and lipid homeostasis and stimulate *Cpt1a*-mediated FA oxidation in a variety of cell types and tissues (19–21). Furthermore, in muscle, GW1516 stimulated FA oxidation due, in part, to increased AMPK activity (26, 27). In a model of hepatic steatosis, GW1516 prevented diet-induced inactivation of hepatic AMPK (24). This suggests that AMPK activation by PPARδ agonists has the ability to regulate hepatic β-oxidation and/or FA synthesis.

The objective of this study was to determine whether PPARδ activation can reverse preestablished hepatic steatosis and insulin resistance. We demonstrate that intervention with GW1516 in $Ldlr^{-/-}$ mice fed a high-fat, cholesterol-containing (HFHC) diet decreased hepatic lipid deposition, a result of attenuated lipogenesis, and increased FA oxidation. Decreased FA synthesis was due to GW1516-mediated correction of selective hepatic insulin resistance. In addition, we provide evidence that AMPK activation was required for the PPARδ-mediated attenuation of hepatic de novo lipogenesis but was not required for PPARδ-mediated induction of FA oxidation. Furthermore, reduced liver TG content was coupled to attenuated hepatic inflammation.

METHODS

Male $Ldlr^{-/-}$ mice on the C57BL/6 background (Jackson Laboratory, Bar Harbor, MA) were housed in pairs in standard cages at 23°C. The animals were cared for in accordance with the Canadian Guide for the Care and Use of Laboratory Animals. All experimental procedures were approved by the Animal Care Committee at the University of Western Ontario. Mice 10–12 weeks of age (n = 16) were fed ad libitum a purified rodent chow diet (14% of calories from fat; Harlan Teklad TD8604, Madison, WI) for 12 weeks. Another group of mice (10–12 weeks of age, n = 48) were fed an HFHC Western diet (42% of calories from fat, 0.2% cholesterol; Harlan Teklad TD09268) for 4 weeks. For the subsequent 8 weeks, half of these mice (n = 24) remained on the HFHC diet; the other half (n = 24) were fed the HFHC diet supplemented with 3 mg/kg/day GW1516 (Enzo Life Sciences, Ann Arbor, MI). A similar dose of GW1516, administered by oral gavage, has been used previously in mice (24, 28, 29). In the present study, at the end of the dark cycle and light cycle, nonfasting

serum concentrations of GW1516 were 604 ± 72 nM and 369 ± 26 nM, respectively, for a mean concentration of 487 ± 50 nM. This plasma concentration is above the EC_{50} for murine PPARδ (20 nM), but below the EC_{50} for murine PPARγ (1 μM) and well below the EC_{50} for murine PPARα (2.5 μM) (30). Animals were fasted for 4 h prior to analyses or being euthanized. For fasting/refeeding studies, animals were either fasted for 16 h prior to being euthanized or fasted for 16 h followed by a 2 h acute refeeding period of the experimental diets prior to being euthanized (31). Blood samples were obtained as previously described (9, 32). Body weights and caloric consumption were determined as described previously (8).

Activation of AMPK in vivo

Activation of AMPK in vivo was assessed in chow-fed *Ldlr*$^{-/-}$ mice following intraperitoneal injection of GW1516 or A-769662 (Selleck Bio, Houston, TX). Animals were fasted overnight (15:00–07:00 h), followed by a period of free access to food (chow) at 07:00 h for 2 h. At 09:00 h, chow was removed and mice were injected intraperitoneally with vehicle (5% dimethyl sulfoxide in PBS), 3 mg/kg GW1516, or 30 mg/kg A-769662, a synthetic activator of AMPK (33). Analyses of in vivo phosphorylation of AMPK and ACC were performed in liver samples isolated at euthanization by a freeze-clamp method, 90 min after injection of the respective treatments, and stored at −80°C until analysis as described (34).

Energy expenditure

In the induction/intervention studies (week 11), analyses of energy expenditure (EE) and respiratory exchange ratio (RER) were performed using the Oxymax Comprehensive Lab Animal Monitoring System (CLAMS, Columbus Instruments, Columbus, OH) (8). Mice were provided free access to food and water and acclimatized to the system for 24 h prior to a 24 h data collection period, during which data on O_2 consumption and CO_2 production were collected every 10 min. EE and RER were calculated as described previously (8).

Primary mouse hepatocyte isolation, lipogenesis, and FA oxidation

Primary mouse hepatocytes were isolated from chow-fed WT or *AMPKβ1*$^{-/-}$ C57BL/6J mice by the collagenase perfusion method as described (35). AMPKβ1 subunit null mice on a C57BL/6 background were generated using standard homologous recombination techniques, as described previously (35, 36). *AMPKβ1*$^{-/-}$ mice have a 90% reduction in liver AMPK activity, compared with WT mice. Studies in primary hepatocytes from *AMPKβ1*$^{-/-}$ mice were conducted by Dr. L. A. Bojic in the laboratory of Dr. G. R. Steinberg, McMaster University (Hamilton, Ontario, Canada). Experiments were performed the day following hepatocyte isolation. For mRNA expression analyses, hepatocytes were incubated with either vehicle, GW1516, or A-769662 (at the indicated concentrations) for 6 h prior to cell lysis in TRIzol® reagent (Life Technologies, Burlington, Ontario, Canada). For lipogenesis and FA oxidation experiments, cells were washed with PBS and incubated in serum-free Medium 199 for 3 h. Lipogenesis was assessed by incubating cells for 4 h with serum-free Medium 199 containing [1-^{3}H]acetate (0.5 μCi/ml) (Amersham Biosciences) and 0.5 mM unlabeled sodium acetate, with or without GW1516 (100 nM) or A-769662 (100 μM). Subsequently, cells were washed twice with PBS and harvested by scraping cells into PBS. Lipids were extracted using the Bligh and Dyer method as described (37, 38). For FA oxidation, cells were incubated for 4 h with serum-free Medium 199 containing [1-^{14}C]palmitic acid (0.5 μCi/ml) (Amersham Biosciences) and 0.5 mM unlabeled palmitate, with or without GW1516 (100 nM) or A-769662 (100 μM). FA oxidation was determined by measuring labeled CO_2 and acid-soluble metabolites as described (39).

Plasma, blood, and tissue analyses

Plasma insulin concentrations were determined by ELISA (Alpco Diagnostics, Salem, NH) in EDTA plasma according to the manufacturer's instructions as described previously (10). Blood glucose was determined using an Ascensia Elite glucometer

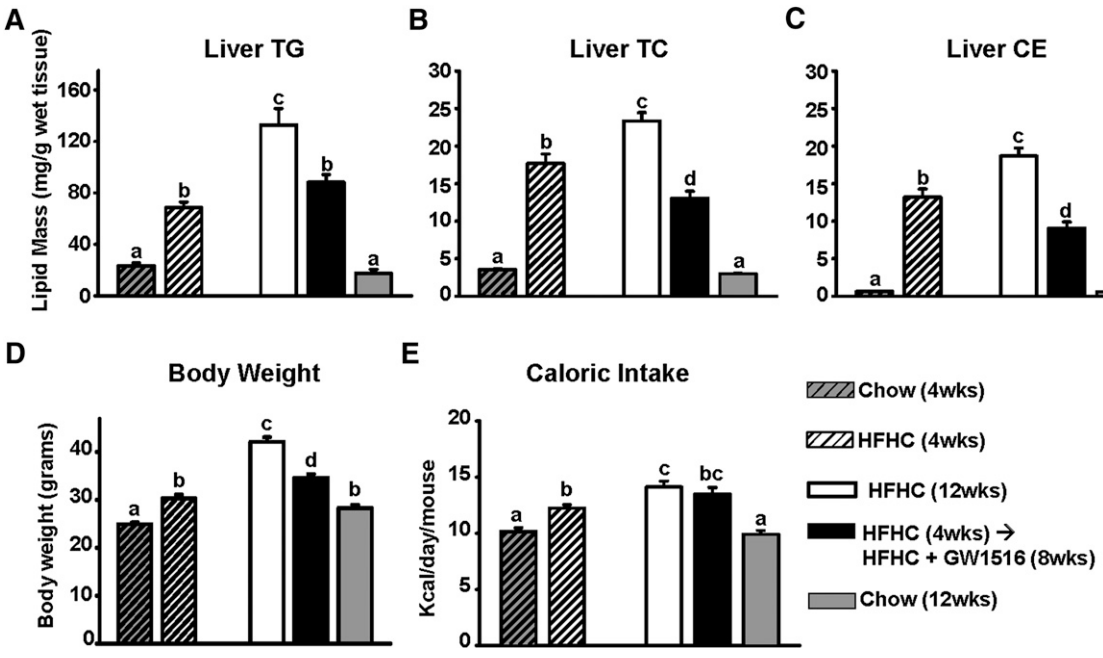

Fig. 1. GW1516 attenuates diet-induced hepatic steatosis and body weight gain, without change in caloric intake. *Ldlr*$^{-/-}$ mice were fed an HFHC diet for 4 weeks. For a subsequent 8 weeks, mice remained on HFHC alone or HFHC supplemented with GW501516 (GW1516) (3 mg/kg/day) (n = 12/group). A: Hepatic TG. B: Hepatic TC. C: Hepatic CE mass. D: Body weight. E: Caloric intake. Data are presented as mean ± SEM. Different letters indicate significant differences; one-way ANOVA with post hoc Tukey's test ($P < 0.05$).

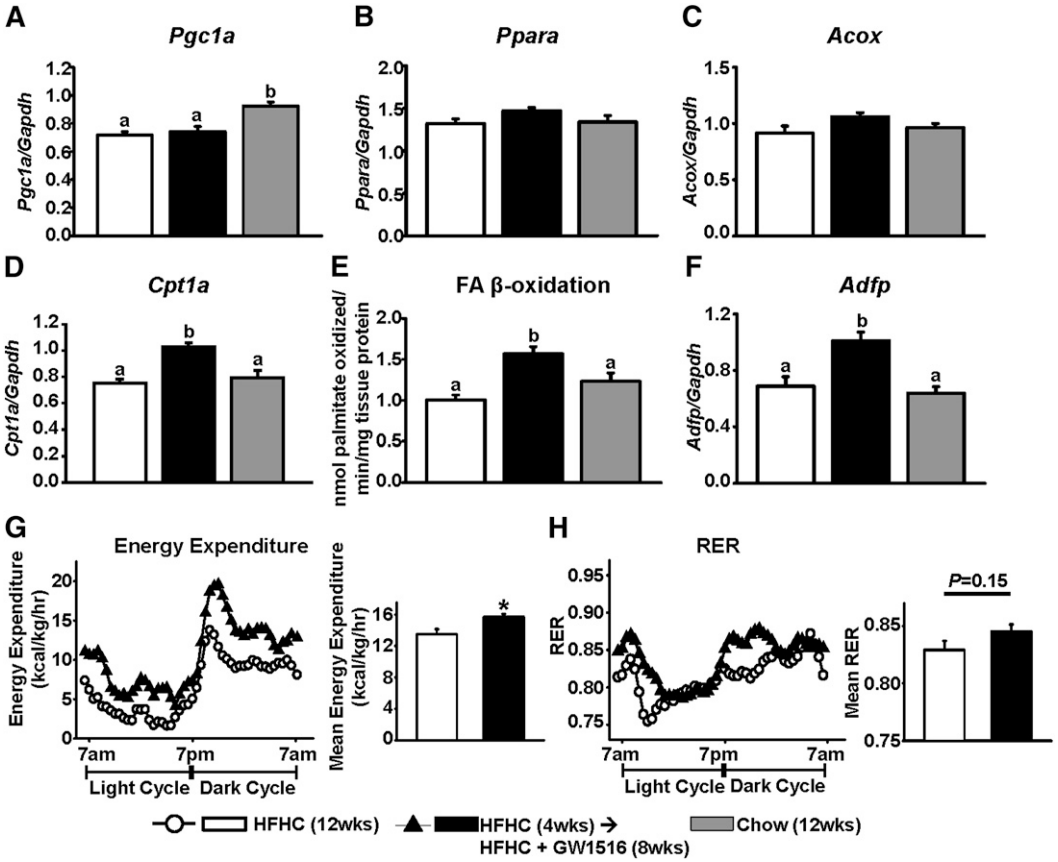

Fig. 2. GW1516 increases hepatic FA oxidation and whole-body EE. Abundance of hepatic *Pgc1a* (A), *Ppara* (B), *Acox* (C), *Cpt1a* (D), and *Adfp* (F) was measured via quantitative real-time PCR and normalized to *Gapdh*. E: Hepatic FA β-oxidation was determined as conversion of [^{3}H]palmitate to ^3H_2O. EE (G) and RER (H) (RER = VO_2/VCO_2) were measured by indirect calorimetry (CLAMS) during a 24 h period. Measurements were collected every 10 min. Mean of each parameter during the 24 h period is shown. Data are presented as mean ± SEM. Different letters indicate significant differences; one-way ANOVA with post hoc Tukey's test ($P < 0.05$). Asterisk (*) indicates significant different between two groups; Student's paired *t*-test ($P < 0.05$).

(Bayer Healthcare, Toronto, Ontario, Canada) (10). Liver lipids were extracted from 100 mg of tissue using the method of Folch et al. (40) and quantitated as described previously (8). FA synthesis was measured following intraperitoneal injection of [1-^{14}C] acetic acid as described (9). Hepatic FA oxidation was determined in tissue homogenates of fresh liver by conversion of [^{3}H] palmitate to ^3H_2O (9).

Immunoblotting and densitometry

Total tissue or cell lysates were isolated from mouse liver or from primary mouse hepatocytes as previously described (41, 42). Proteins were separated by SDS-PAGE, transferred to polyvinylidene difluoride (PVDF) membranes, and immunoblotted (42). Membranes were probed using antibodies against mouse phosphorylated and total Akt, FoxO1, mTOR, AMPK, and ACC, as well as 78 kDa glucose-regulated protein (GRP78), CCAAT/enhancer binding protein-homologous protein (CHOP), and β-actin (Cell Signaling, Danvers, MA). The anti-phosphorylated ACC antibody recognizes both pACC1 Ser76 and pACC2 Ser212, which recently have been shown to have overlapping functions (43). For SREBP-1, liver lysates were separated into postnuclear and nuclear fractions as described (41, 42). Each fraction was separated by SDS-PAGE (4–15% acrylamide gradient) and transferred to PVDF membranes (42). Membranes from both fractions were probed with a monoclonal antibody to SREBP-1 (Neomarkers, Fremont, CA), stripped, and reprobed with either the β-actin antibody for the postnuclear fraction or a polyclonal lamin A/C antibody (Santa Cruz Biotechnology, Santa Cruz, CA) for the nuclear fraction (41). Quantitation of protein on all blots was determined by densitometry as described (41, 42).

Quantitative real-time PCR gene abundance analyses

Total RNA was isolated from liver tissue or primary mouse hepatocytes using TRIzol® reagent as per the manufacturer's instructions. Specific mRNA abundances [PPAR gamma coactivator 1a (*Pgc1a*), *Ppara*, *Acox*, *Cpt1a*, adipocyte differentiation-related protein (*Adfp*), sterol-regulatory element binding factor 1c (*Srebf1c*), *Fasn*, insulin-induced gene 1 (*Insig1*), insulin-induced gene 2a (*Insig2a*), phosphoenolpyruvate carboxykinase 1 (*Pck1*), *Tnf*, intercellular adhesion molecule 1 (*Icam1*), interleukin 1b (*Il1b*), chemokine (C-C motif) ligand 2 (*Ccl2*), chemokine (C-C motif) ligand 3 (*Ccl3*), inducible NO synthase (*iNos*), arginase 1 (*Arg1*), heat shock 70kDa protein 5 (*Hspa5*), and *Gapdh*] were measured via quantitative real-time PCR using an ABI Prism (7900HT) Sequence Detection System (Applied Biosystems, Foster City, CA) as previously described (9, 44). mRNA abundances were calculated using the standard curve method. Primer and probe sets were obtained from Applied Biosystems (Streetsville, CA) inventoried gene expression arrays with the exception of murine *Srebf1c* (*Srebp1c*), which was generated as described previously (9, 44).

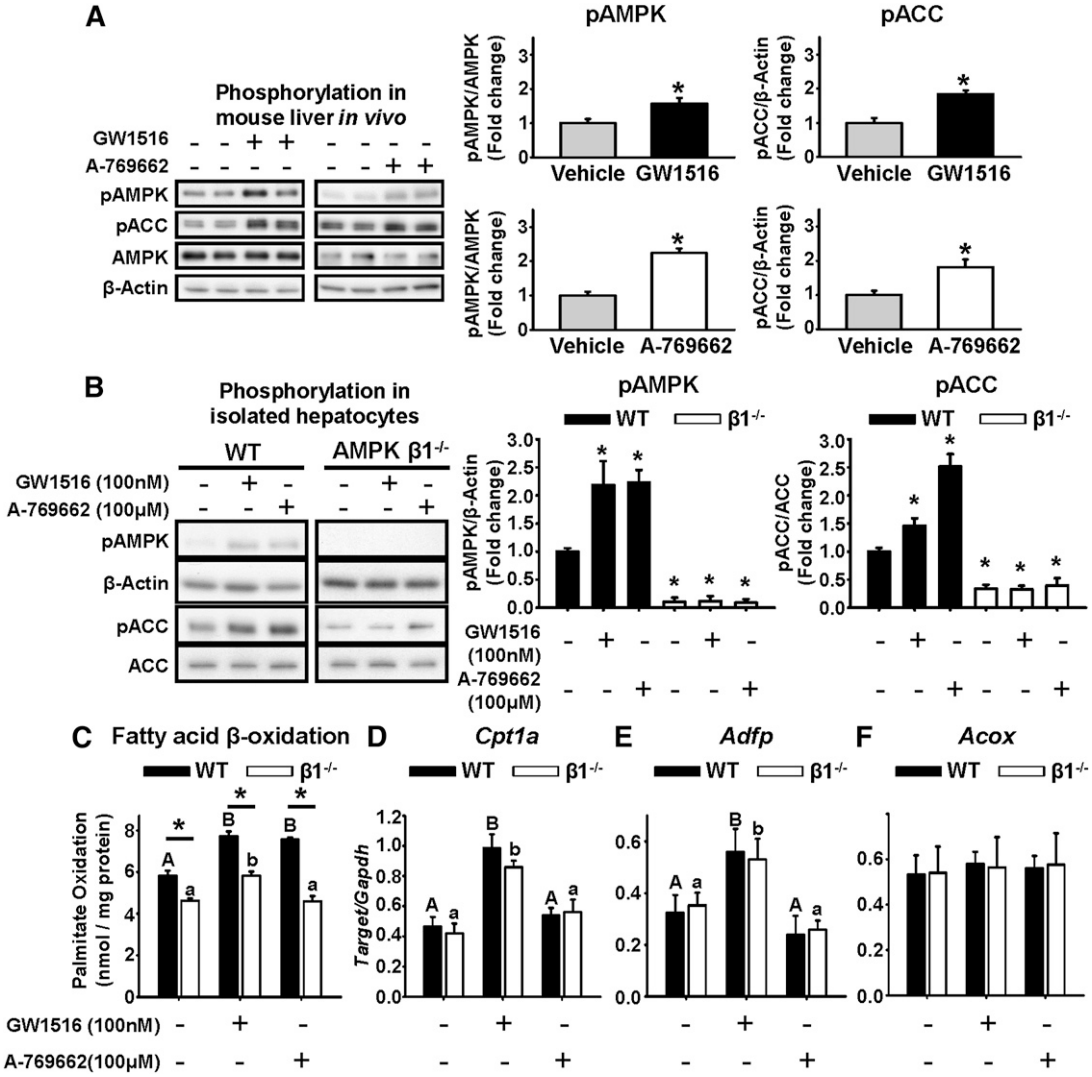

Fig. 3. GW1516 increases AMPK and ACC phosphorylation, which is not required for FA oxidation. A: Eight- to 10-week-old *Ldlr*$^{-/-}$ mice fed a standard laboratory chow were fasted overnight, fed at 07:00 h for 2 h, and refasted at 09:00 h. Intraperitoneal injection of vehicle, GW1516 (3 mg/kg), or A-769662 (30 mg/kg) (n = 6/group) occurred at the beginning of the refasting period at 09:00 h. Immunoblots of AMPK and ACC in freeze-clamped liver lysates 90 min postinjection. Representative immunoblots with quantitations are shown. Asterisk (*) indicates significant difference between vehicle and treatment; Student's paired *t*-test ($P < 0.05$). B–F: Primary hepatocytes isolated from WT and AMPKβ1$^{-/-}$ mice. Cells were incubated for 1 h with or without GW1516 or A-769662, and lysates were immunoblotted for phosphorylated AMPK and ACC (pAMPK, pACC) (B). Representative immunoblots with quantitations are shown. Asterisk (*) indicates significant difference versus WT control; Student's paired *t*-test ($P < 0.05$). C: Isolated hepatocytes were treated with 0.5 mM palmitate (0.5 μCi/ml [^{14}C]palmitate) for 4 h with or without GW1516 or A-769662 prior to determination of FA oxidation. In isolated hepatocytes treated with or without GW1516 or A-769662 for 6 h, mRNA abundances of *Cpt1a* (D), *Adfp* (E), and *Acox* (F) were measured by quantitative real-time PCR and normalized to *Gapdh*. Different uppercase letters indicate statistical significance among treatments in WT hepatocytes, different lowercase letters indicate statistical significance among treatments in β1$^{-/-}$ hepatocytes, and an asterisk (*) indicates statistical significance between WT and β1$^{-/-}$ within the same treatment group ($P < 0.05$); two-way ANOVA with post hoc Tukey's test ($P < 0.05$). All data are presented as mean ± SEM (n = 3–4 from at least three independent experiments).

Statistical analyses

Data are expressed as means ± SEM. Student's paired *t*-test was used to determine significant differences between two groups. One-way ANOVA followed by pair-wise comparisons by the Tukey's test was used to determine differences between three or more groups. For fasting/refeeding experiments and experiments involving WT or AMPKβ1$^{-/-}$ primary mouse hepatocytes, two-way ANOVA followed by pair-wise comparisons by the Tukey's test was used to determine statistically significant differences and interactions except for experiments where comparisons are made with WT control. For these, two-way ANOVA followed by the Bonferroni test was used. Significance thresholds were *P* values < 0.05 and marked by different uppercase or lowercase letters as well as asterisks, as indicated in the figure legends.

RESULTS

GW1516 treatment attenuates hepatic TG accumulation, in part, by stimulating FA β-oxidation

Male C57BL/6 *Ldlr*$^{-/-}$ mice were administered an HFHC diet for 4 weeks to induce hepatic steatosis. Subsequently,

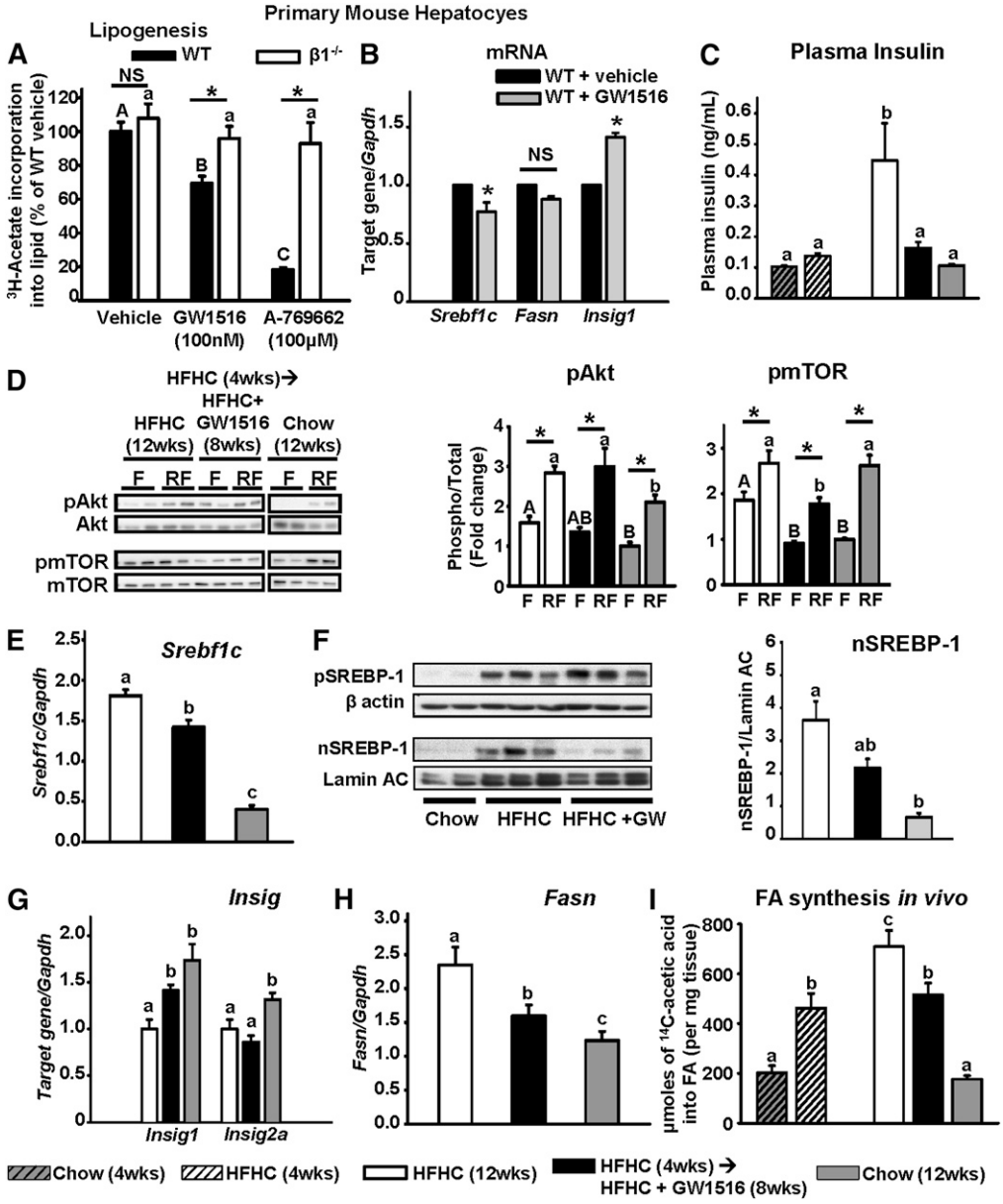

Fig. 4. GW1516 inhibits hepatic FA synthesis as a consequence of AMPK activation and correction of selective hepatic insulin resistance. A: Primary mouse hepatocytes isolated from WT and AMPK$\beta1^{-/-}$ ($\beta1^{-/-}$) mice were incubated with 0.5 mM sodium acetate (0.5 μCi/ml ^{3}H-acetate) for 4 h with or without GW1516 or A-769662 prior to determination of lipogenesis (n = 3–4 from at least three independent experiments). Different uppercase letters indicate statistical significance among WT treatments, different lowercase letters indicate statistical significance among $\beta1^{-/-}$ treatments, and asterisk (*) indicates statistical significance between WT and $\beta1^{-/-}$ within the same treatment group ($P < 0.05$); two-way ANOVA with post hoc Tukey's test ($P < 0.05$). B: Primary hepatocytes isolated from chow-fed WT mice treated with or without GW1516 for 6 h; mRNA abundances of *Srebf1c*, *Fasn*, and *Insig1* were measured by quantitative real-time PCR and normalized to *Gapdh*. Asterisk (*) indicates significant difference to vehicle-treated control; Student's paired *t*-test ($P < 0.05$). C: Plasma insulin at the end of the induction (4 weeks) or intervention (12 weeks) phase in $Ldlr^{-/-}$ mice fasted overnight. Different letters indicate significant differences; one-way ANOVA with post hoc Tukey's test ($P<0.05$). D: Immunoblots of insulin signaling proteins phosphorylated Akt and mTOR (pAkt, pmTOR) in liver lysates from $Ldlr^{-/-}$ mice fasted overnight (designated F) or fasted overnight followed by a 2 h refeeding period (designated RF). Representative immunoblots with quantitations are shown. Different uppercase letters indicate statistical significance among fasted animals, different lowercase letters indicate statistical significance among refed animals, and asterisk (*) indicates statistical significance between fasted and refed within the same diet group ($P < 0.05$); two-way ANOVA with post hoc Tukey's test ($P < 0.05$). mRNA abundance of *Srebf1c* (E), *Insig1* and *Insig2a* (G), and *Fasn* (H) in liver lysates isolated from animals fasted for 4 h (n = 6–8/group). F: Representative immunoblots of SREBP-1 precursor (pSREBP-1) in the postnuclear fraction, and the processed nuclear form (nSREBP-1) in the nucleus of liver lysates isolated from $Ldlr^{-/-}$ mice fasted for 4 h. Quantitation of nSREBP-1 blots relative to lamin A/C (n = 5/group)

mice were fed the HFHC diet supplemented with either vehicle or GW1516 (3 mg/kg/day) for an additional 8 weeks. In mice fed the HFHC diet for 4 weeks, prominent hepatic steatosis developed, as evidenced by significantly increased TG, total cholesterol (TC), and cholesteryl ester (CE) (**Fig. 1A–C**). These lipids continued to increase over the subsequent 8 weeks in HFHC-fed mice. In contrast, the addition of GW1516 to the HFHC diet for 8 weeks decreased hepatic lipids by 30–50% demonstrating a significant slowing of steatosis progression (Fig. 1A–C). As we reported previously using a similar protocol (45), GW1516 intervention reduced the rate of weight gain (−60%), whereas caloric consumption was unaffected (Fig. 1D, E).

We reasoned that GW1516 attenuates liver TG accumulation via increased FA β-oxidation and/or reduced FA synthesis. With respect to FA oxidation, suppressed *Pgc1a* expression in livers of mice fed the HFHC diet for 12 weeks (−20% compared with chow-fed mice) was not further affected by GW1516 treatment (**Fig. 2A**). Furthermore, at 12 weeks, the expression of *Ppara* and the PPARα-target gene *Acox* was unaffected by any diet (Fig. 2B, C). In contrast, *Cpt1a* mRNA abundance was significantly enhanced (35%) in livers isolated from GW1516-treated animals, which was associated with a significant 50% increase in FA oxidation as compared with HFHC-fed animals (Fig. 2D, E). Expression of the PPARδ-specific target gene *Adfp* (46) was significantly increased (∼60%) in livers from GW1516-treated animals (Fig. 2F). Collectively, these results suggest that GW1516 attenuates liver TG accumulation partly due to increased hepatic FA β-oxidation, primarily the consequence of activating the PPARδ-target gene *Cpt1a*.

To further investigate the GW1516-induced increase in hepatic FA oxidation, we assessed energy balance in a metabolic monitoring system. Total EE was significantly higher (16%) in mice receiving GW1516 compared with mice remaining on the HFHC diet alone (Fig. 2G). The RER profiles, which reflect the relative utilization of carbohydrate (RER ∼1.0) versus fat (RER ∼0.7), were similar between the HFHC-fed and GW1516-intervention groups (Fig. 2H). Given the significant increase in total EE in GW1516-treated mice, the lack of difference in RER profiles suggests that both carbohydrate and fat utilization are increased by PPARδ activation.

AMPK activation is not required for the GW1516-mediated increase in fat oxidation

GW1516 has been shown to activate AMPK in muscle (26). Given the GW1516-induced stimulation of hepatic FA oxidation in vivo, we hypothesized that AMPK activation may be involved. To evaluate the ability of GW1516 to acutely activate hepatic AMPK in vivo, we used a fasting, feeding, injection, and refasting protocol (34). In livers isolated 90 min after the injection of GW1516, we observed a significant 2-fold increase in phosphorylation of AMPK and its downstream effector ACC (**Fig. 3A**). Mice were also injected with the potent synthetic AMPK activator A-769662 (33), which increased AMPK and ACC phosphorylation ∼2-fold (Fig. 3A).

The requirement of AMPK for the GW1516-mediated stimulation of FA oxidation was determined in isolated primary mouse hepatocytes from WT or AMPKβ1$^{-/-}$ mice [referred to as AMPK β1 subunit knockout (β1$^{-/-}$) mice]. Deletion of the AMPKβ1 subunit results in 90% loss of hepatic AMPK activity (35). As depicted in Fig. 3B, both GW1516 and A-769662 increased phosphorylation of AMPK and ACC in WT hepatocytes but not in β1$^{-/-}$ hepatocytes. Furthermore, both GW1516 and A-769662 enhanced FA oxidation in WT hepatocytes by 30% (Fig. 3C). The effect of A-769662 was lost in β1$^{-/-}$ hepatocytes, consistent with an AMPKβ1-dependent effect (36). However, as in WT cells, GW1516 was able to increase FA oxidation in β1$^{-/-}$ hepatocytes by ∼30% (Fig. 3C). To reconcile this, we examined *Cpt1a* expression, a PPARδ-target gene, in WT and β1$^{-/-}$ hepatocytes. GW1516-treatment significantly enhanced *Cpt1a* expression (∼2-fold) in both WT and β1$^{-/-}$ hepatocytes (Fig. 3D). In contrast, A-769662 had no effect on *Cpt1a* mRNA abundance in hepatocytes of either genotype (Fig. 3D). The PPARδ-specific target gene *Adfp* was increased 2-fold in isolated hepatocytes from either genotype, whereas the PPARα-specific target *Acox* was unaffected by genotype or treatment (Fig. 3E, F). Taken together, these results demonstrate that the GW1516-induced increase in *Cpt1a*-mediated FA oxidation does not require AMPK activation and does not involve PPARα activation.

GW1516 intervention attenuates de novo lipogenesis, in part, via activation of AMPK as well as correction of selective hepatic insulin resistance

In addition to regulating FA oxidation, AMPK is known to regulate de novo lipogenesis (14). When incubated with WT hepatocytes, GW1516 significantly inhibited de novo lipogenesis by ∼30% (**Fig. 4A**). This effect was significantly attenuated in β1$^{-/-}$ hepatocytes (Fig. 4A). Consistent with an AMPKβ1-specific effect, the 80% reduction in lipogenesis by A-769662 in WT hepatocytes was lost in β1$^{-/-}$ hepatocytes (Fig. 4A). In WT hepatocytes, GW1516 decreased the expression of *Srebf1c* (−24%) and *Fasn* (−18%, not significant) and increased the expression of *Insig1* (40%) (Fig. 4B). Increased expression of the PPARδ-target gene *Insig1* has been shown to inhibit the processing of SREBP-1 to its active nuclear form (nSREBP-1) (23). Together, these data demonstrate that in isolated hepatocytes, GW1516 inhibits de novo lipogenesis through activation of AMPK.

In vivo, selective hepatic insulin resistance contributes to FA synthesis due to hyperinsulinemia-driven mTORC1 activation of SREBP-1c (4). As we reported previously (45), the HFHC diet resulted in continued progression of

is shown. Different letters indicate significant differences; one-way ANOVA with post hoc Tukey's test ($P < 0.05$). I: Synthesis of FA in liver obtained 60 min postinjection (intraperitoneal) with [^{14}C]acetic acid (n = 6–8/group). Different letters indicate significant differences; one-way ANOVA with post hoc Tukey's test ($P < 0.05$). All data are presented as mean ± SEM.

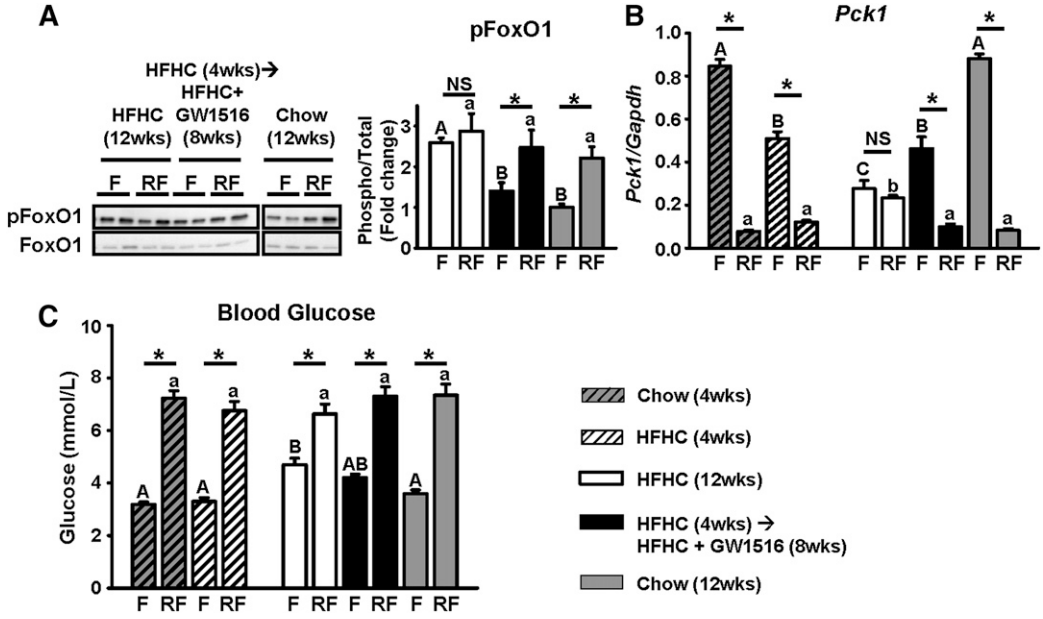

Fig. 5. GW1516 corrects the gluconeogenic branch of insulin signaling during selective hepatic insulin resistance, which improves fasting hyperglycemia. A: Immunoblots of insulin signaling protein pFoxO1 in liver lysates from fasted (F) and refed (RF) mice (n = 6–8/group). Representative immunoblots with quantitations are shown. B: mRNA abundance of *Pck1* in liver lysates isolated from F and RF animals (n = 6–8/group). C: Blood glucose levels in F and RF mice (n = 6–8/group). Data are presented as mean ± SEM. Different uppercase letters indicate statistical significance among fasted animals, different lowercase letters indicate statistical significance among refed animals, and asterisk (*) indicates statistical significance between fasted and refed within the same diet group ($P < 0.05$); two-way ANOVA with post hoc Tukey's test ($P < 0.05$).

fasting hyperinsulinemia throughout the study (Fig. 4C). Fasting hyperinsulinemia was strongly attenuated by intervention with GW1516 to the HFHC diet (Fig. 4C). Selective hepatic insulin resistance was evaluated using a fasting (16 h)/refeeding (2 h) protocol. Compared with chow-fed mice, phosphorylation of hepatic Akt was significantly elevated in the fasted state in HFHC-fed mice, and the response to feeding was enhanced (Fig. 4D). A similar pattern for pAkt was observed in GW1516-treated mice. However, in HFHC-fed mice, the phosphorylation of mTORC1 was elevated in the fasted state, and the response to feeding was exaggerated. In contrast, GW1516 intervention completely restored the fasting/refeeding responses of pmTORC1 to levels observed in chow-fed controls (Fig. 4D). This is consistent with increased sensitivity in the lipogenic mTORC1 branch of the insulin signaling cascade in HFHC-fed mice (4) and its normalization following GW1516 treatment.

Compared with chow-fed controls, the hyperinsulinemia and increased hepatic pmTORC1 observed in fasted HFHC-fed mice at 12 weeks was associated with increased expression of *Srebf1c*, increased nSREBP-1, decreased expression of both *Insig1* and *Insig2a*, and increased expression of *Fasn* (Fig. 4E–H), as well as markedly enhanced FA synthesis (Fig. 4I). GW1516-intervention attenuated the expression of *Srebf1c*, inhibited formation of nSREBP-1, and increased the expression of the PPARδ-target gene *Insig1* (Fig. 4E–G), which is known to block processing of SREBP-1c (23). The expression of *Insig2a*, which is dependent on Akt signaling (7), was unaffected by GW intervention (Fig. 4G). Reduced nSREBP-1 was associated with a decrease in *Fasn* expression (Fig. 4F, H) and was coupled to a complete inhibition of the HFHC-induced increase in FA synthesis from 4 to 12 weeks of GW1516 intervention (Fig. 4I). Together with results in primary mouse hepatocytes, these data indicate that PPARδ activation inhibits hepatic lipogenesis through activation of AMPK as well as correction of selective hepatic insulin resistance, both of which contribute to the attenuation of liver TG accumulation.

PPARδ activation restores dynamic regulation of hepatic FoxO1, which slows the development of hyperglycemia

Given that PPARδ activation improves hepatic insulin sensitivity in *db/db* mice (19), we hypothesized that the GW1516-mediated correction of the HFHC diet-induced bifurcation in hepatic insulin signaling would normalize FoxO1 signaling. At 12 weeks, livers isolated from HFHC-fed mice lost the ability to stimulate FoxO1 phosphorylation and suppress *Pck1* expression in the fasting-to-feeding transition (**Fig. 5A, B**). This is consistent with our previous hyperinsulinemic euglycemic clamp studies in which the livers of $Ldlr^{-/-}$ mice fed a high-fat diet were insulin resistant (10). In contrast, animals receiving the GW1516 intervention regained the ability to dynamically regulate fasting/refeeding of both FoxO1 phosphorylation and *Pck1* expression, similar to that observed in chow-fed mice (Fig. 5A, B). As we reported previously (45), fasting blood glucose levels were increased (1.5-fold) in mice fed HFHC for 12 weeks, which was partially attenuated by GW1516 intervention (Fig. 5C).

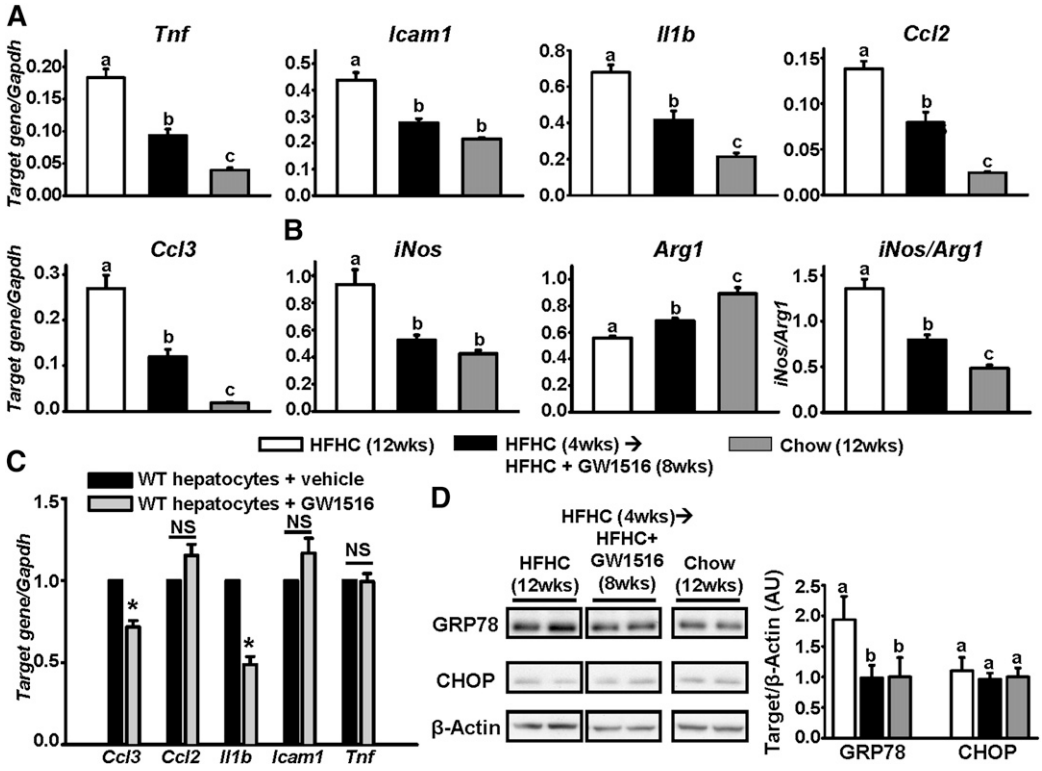

Fig. 6. GW1516 attenuates hepatic inflammation and markers of ER stress. $Ldlr^{-/-}$ mice were fed an HFHC diet for 4 weeks. For a subsequent 8 weeks, mice remained on HFHC alone or supplemented with GW501516 (GW1516) (3 mg/kg/day) (n = 12/group). A, B: Hepatic abundance of cytokines was determined at 12 weeks by quantitative real-time PCR, and expression was normalized to *Gapdh*. C: Primary hepatocytes isolated from chow-fed WT mice treated with or without GW1516 for 6 h. mRNA abundances of *Ccl3*, *Ccl2*, *Il1b*, *Icam1*, and *Tnf* were measured by quantitative real-time PCR, expressed relative to *Gapdh* and normalized to untreated cells. Asterisk (*) indicates significant difference to vehicle-treated control; Student's paired *t*-test ($P < 0.05$). D: Immunoblots of GRP78 and CHOP in liver lysates from $Ldlr^{-/-}$ mice at 12 weeks. Representative immunoblots with quantitations are shown. Data are presented as mean ± SEM (n = 8–12/group). Different letters indicate significant differences; one-way ANOVA with post hoc Tukey's test ($P < 0.05$).

These data suggest that the abnormal gluconeogenic branch of insulin signaling, resulting from diet-induced selective hepatic insulin resistance, is corrected by intervention with GW1516, leading to improved fasting blood glucose concentrations.

GW1516 inhibits hepatic inflammation and induction of endoplasmic reticulum stress

Inflammation is a prominent feature of hepatic insulin resistance and steatosis (3). Given that GW1516 intervention attenuated hepatic steatosis and corrected selective hepatic insulin resistance, we postulated that this would be associated with reduced hepatic inflammation. As shown in **Fig. 6A, B**, expression of the proinflammatory M1 cytokines *Tnf*, *Icam1*, *Il1b*, *Ccl2*, *Ccl3*, and *iNos* was markedly induced (2- to 15-fold) in livers of mice fed the HFHC diet at 12 weeks. In contrast, these cytokines were significantly attenuated (−50 to −65%) in livers from the GW1516-intervention group (Fig. 6A, B). Furthermore, HFHC feeding strongly suppressed hepatic expression of the M2 anti-inflammatory marker *Arg1*, resulting in a greatly exacerbated *iNos/Arg1* ratio compared with chow-fed control mice (Fig. 6B). GW1516 intervention reversed or completely prevented this expression pattern (Fig. 6B). Together these data suggest that PPARδ activation promotes an anti-inflammatory M2 cytokine milieu in the liver. To assess the direct effect of GW1516 on the inflammatory response, we examined the expression of inflammatory genes in primary hepatocytes from chow-fed mice incubated with GW1516. Of the cytokines examined, the expression of *Ccl3* (−25%) and *Il1b* (−50%) were significantly decreased (Fig. 6C). A similar response of these two cytokines to GW1516 was reported in cultured macrophages (47), suggesting that a direct effect of GW1516 on the expression of *Ccl3* and *Il1b* contributed to their decreased expression in liver following GW intervention (Fig. 6A). Furthermore, it is likely that the attenuated hepatic expression of *Tnf*, *Icam1*, and *Ccl2* were the consequence of reduced hepatic steatosis.

Inflammation is commonly interwoven with endoplasmic reticulum (ER) stress in the development of hepatic insulin resistance (3, 48). Accordingly, HFHC feeding significantly increased hepatic GRP78 (Fig. 6D), a marker of the unfolded protein response (UPR), which is the precursor to the ER-stress response (49). GW1516 intervention completely normalized the diet-induced increase in

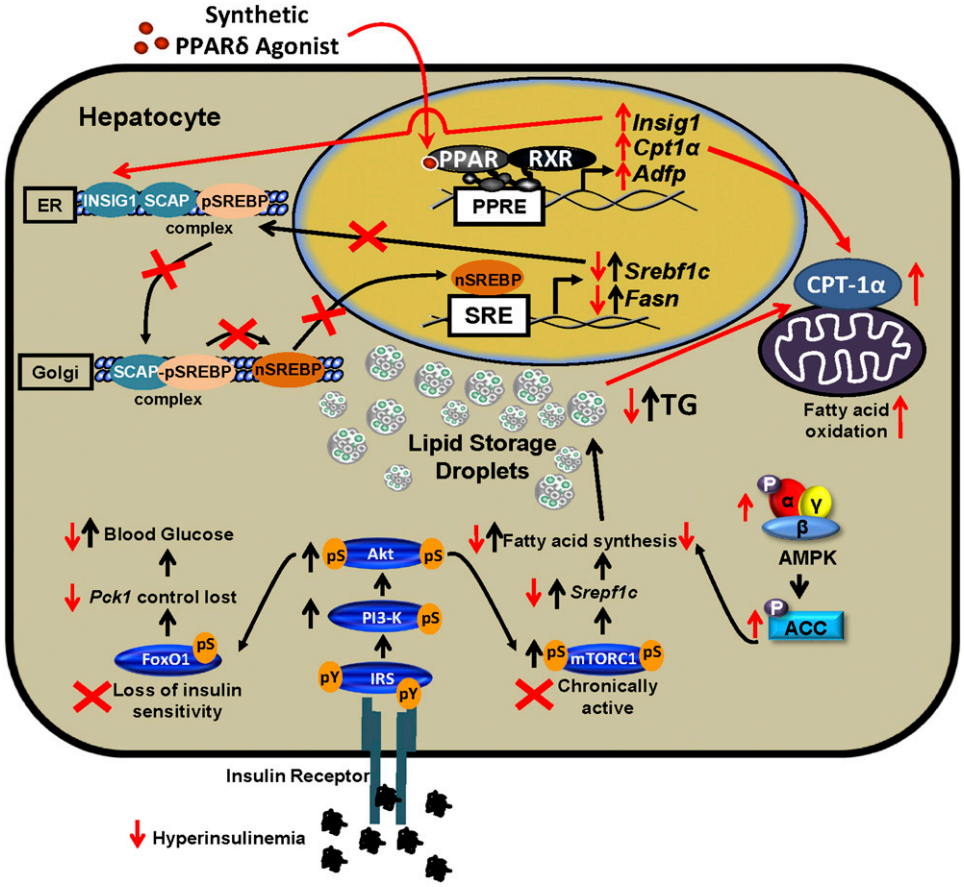

Fig. 7. GW1516 intervention inhibits progression of hepatic steatosis in mice. Selective insulin resistance in the liver is induced in mice fed a high-fat diet. Despite hyperinsulinemia, insulin fails to decrease gluconeogenesis due to resistance of the FoxO1 pathway (loss of fasting/refeeding regulation of phospho-serine, pS), whereas the mTORC1/SREBP-1c pathway maintains insulin sensitivity (fasted pS-mTOR is elevated and increased even further with refeeding), leading to increased FA synthesis and TG accumulation. Pathways affected by diet are denoted by black arrows. Red arrows and crosses indicate the effects of GW1516 intervention. PPARδ activation attenuated hepatic TG accumulation as a consequence of increased FA oxidation and reduced FA synthesis. GW1516 stimulated FA oxidation due to increased *Cpt1a* expression. Increased hepatic AMPK activation by GW1516 was, in part, required for reduction of FA synthesis. The PPARδ agonist suppressed hyperinsulinemia, corrected signaling through the FoxO1 pathway, and normalized signaling through the mTORC1/SREBP-1c pathway. GW1516 decreased *Srebf1c* expression and inhibited the conversion of precursor SREBP-1c (pSREBP-1c) to the active nuclear form (nSREBP-1c), in part, due to increased expression of *Insig1*, which collectively contributed to the decreased FA synthesis. PPRE, PPAR response element; SCAP, SREBP cleavage-activating protein; SRE, sterol response element.

GRP78 (Fig. 6D). CHOP, the downstream effector of the ER-stress response, was not increased by the HFHC diet, nor was it affected by GW1516 (Fig. 6D). This suggests that although the HFHC diet initiated the UPR, GRP78 expression was sufficient to prevent the full downstream ER-stress response. Nevertheless, PPARδ activation attenuated the HFHC diet-induction of the UPR. The expression of *Hspa5*, which codes for GRP78, was unaffected by GW1516 in primary hepatocytes (data not shown), suggesting that the GW-induced reduction in GRP78 in vivo was secondary to decreased hepatic steatosis.

DISCUSSION

We evaluated the ability of the PPARδ agonist GW1516 to attenuate the progression of diet-induced hepatic steatosis. GW1516 intervention inhibited the progression of liver TG accumulation, the consequence of reduced FA synthesis and increased FA oxidation. GW1516 activated hepatic AMPK in vivo and in vitro. Exposure of isolated hepatocytes deficient in AMPK activity to GW1516 revealed that inhibition of lipogenesis required AMPK, whereas the induction of FA oxidation was mediated through increased expression of *Cpt1a*, rather than by AMPK activation. Hepatic lipogenesis was also attenuated through GW1516-mediated correction of selective hepatic insulin resistance, which was associated with reduced hepatic inflammation (**Fig. 7**).

The role of PPARδ activation in liver TG metabolism has been controversial (19, 22–25). One study showed that GW1516 prevented diet-induced suppression of hepatic AMPK activation, which was associated with increased

expression of genes involved in FA oxidation and increased plasma β-hydroxybutyrate (24). Despite these observations, GW1516 did not affect hepatic TG content (24). Another study demonstrated that injection of ad*PPARδ* into *Ldlr*$^{-/-}$ mice significantly increased hepatic AMPK phosphorylation, which was thought to contribute to glucose lowering (25). However, the impact of increased hepatic AMPK activation on lipid metabolism was not explored (25). Here we provide direct evidence that PPARδ activation increases hepatic AMPK and ACC phosphorylation in vivo as well as in primary mouse hepatocytes. It is possible that this effect was due to changes in adenylate charge (24). Nevertheless, the GW1516-mediated increase in pACC was AMPK dependent as this effect was lost in β1$^{-/-}$ hepatocytes. We demonstrate that PPARδ activation stimulates hepatic FA oxidation in vivo through PPARδ-specific activation of *Cpt1a*. We recapitulated these results in primary mouse hepatocytes and showed that AMPK activation is not a requirement for GW1516-induced FA oxidation, as enhanced *Cpt1a* expression and FA oxidation persisted in GW1516-treated β1$^{-/-}$ hepatocytes.

Studies that have examined the role of PPARδ activation in hepatic de novo lipogenesis have yielded both positive and negative results (19, 23, 25). On one hand, both ad*PPARδ* injection and GW1516 treatment have been shown to increase hepatic expression of genes involved in lipogenesis, resulting in increased liver TG accumulation (19, 25). On the other hand, delivery of ad*PPARδ* or the synthetic PPARδ agonist GW0742 have demonstrated reduced SREBP-1c processing, decreased lipogenic gene expression, and prevention of hepatic steatosis (23). The data presented here are consistent with and extend this latter concept. We provide evidence that intervention to an HFHC diet with GW1516 in mice halts progression of hepatic steatosis and corrects selective hepatic insulin resistance by normalizing signaling through mTORC1, resulting in suppression of lipogenic gene expression. Not only was *Srebf1c* expression decreased, but processing of SREBP-1 to its active nuclear form was inhibited. The GW1516-induced expression of *Insig1* likely contributes to this inhibition (23). Other insulin-regulated factors known to influence SREBP-1 processing were either unchanged (*Insig2a*) or were not examined (Gsk3B and Lipin1) (7, 23, 50). Collectively, the GW1516-induced suppression of the SREBP-1c pathway contributed to the prevention of any further increase in FA synthesis. Furthermore, GW1516 reduced de novo lipogenesis in WT primary mouse hepatocytes, but not in β1$^{-/-}$ hepatocytes, demonstrating that inhibition of FA synthesis was AMPK dependent. Although two different mechanisms contribute to the observed reduction in lipogenesis by GW1516 treatment, the relative contributions of these pathways require further study.

Coupled to hyperinsulinemia, the bifurcation in insulin signaling, in which FoxO1 becomes insulin resistant and the mTORC1/SREBP-1c pathway maintains insulin sensitivity, contributes to hepatic steatosis, dyslipidemia, and hyperglycemia (4). In the present study, we provide evidence that hepatic insulin signaling does in fact bifurcate in a model of diet-induced insulin resistance. Importantly, we demonstrate that PPARδ activation attenuates the progression of the selective hepatic insulin-resistant phenotype, as dynamic regulation of fasting-to-feeding pmTORC1, pFoxO1, and *Pck1* expression was restored in the GW1516-intervention cohort. These data elaborate on the body of evidence that PPARδ activation not only protects from insulin resistance (19–21), but can also reverse preestablished hepatic insulin resistance.

Liver inflammation has been linked to hepatic steatosis and insulin resistance (3, 51). Vascular chronic low-grade inflammation is, in part, mediated by aortic lipid accumulation and insulin resistance (52, 53). Given the selective insulin-resistant phenotype and TG acquisition in livers of HFHC-fed animals and correction by GW1516 intervention, it is tempting to hypothesize that similar mechanisms govern induction and attenuation of vascular and hepatic inflammation. Moreover, Kupffer cell-specific deletion of *Ppard* in mice resulted in increased proinflammatory cytokine expression and reduced anti-inflammatory cytokine expression, which was coupled to increased liver TG accumulation and hepatic dysfunction (54). Therefore, our results are consistent with an anti-inflammatory role for PPARδ activation in the liver, similar to the effect in macrophages and in the aorta (28, 45, 47). The relative impact of reduced inflammation versus correction of insulin sensitivity to the attenuation of hepatic steatosis cannot be discerned from the present experiments and requires further elucidation.

Previous studies raise the possibility that the reduction in hepatic steatosis with GW1516 intervention was an indirect consequence of attenuated body weight gain or the small decrease in adipose tissue mass (~10%) (45), as GW1516 is known to also target adipose tissue (21). Wang et al. (21) reported that adipose tissue-specific overexpression (3-fold) of a *PPARD* expression vector in HFD-fed C57BL/6 mice decreased adiposity (~50%), primarily due to an increase in adipocyte *Cpt1a* expression and enhanced FA oxidation. This was associated with a decrease in lipid droplets within liver sections. Using a similar approach, Qin et al. (23) reported that hepatic overexpression of PPARδ following injection of *PPARD* adenovirus in *db/db* mice suppressed the hepatic expression of genes involved in FA synthesis, decreased SREBP-1c processing, and attenuated Oil Red O-stained hepatic lipid. Although neither FA oxidation nor insulin resistance were measured, these latter results are consistent with the concept that direct hepatic activation of PPARδ is able to attenuate hepatic steatosis.

In the present study, we show in primary mouse hepatocytes from chow-fed mice and in liver from HFHC-fed mice that PPARδ activation by GW1516 increases the expression of the PPARδ-specific target gene *Adfp*. Furthermore, the PPARδ-target gene *Cpt1a* was increased directly or consequent to PPARδ-induced AMPK activation, leading to increased FA oxidation. In addition, GW1516 suppressed lipogenesis in hepatocytes and liver due to activation of AMPK and phosphorylation of ACC, as well as decreased expression of *Srebf1c*, and suppression of SREBP-1 processing to its active nuclear form. The latter was associated with increased expression of *Insig1*, considered to be a direct

target of PPARδ (23). These results suggest that the attenuation of hepatic steatosis and improved hepatic insulin signaling are the consequence of a direct effect of GW1516 within the liver.

In summary, the data reported here provide physiological and molecular evidence that intervention with PPARδ-specific activation in the liver alleviates diet-induced hepatic steatosis, insulin resistance, and inflammation. We conclude that PPARδ agonists may serve as therapeutic options for the treatment of patients with hepatic steatosis.

REFERENCES

1. Farese, R. V., Jr., R. Zechner, C. B. Newgard, and T. C. Walther. 2012. The problem of establishing relationships between hepatic steatosis and hepatic insulin resistance. *Cell Metab.* **15:** 570–573.
2. Williamson, R. M., J. F. Price, S. Glancy, E. Perry, L. D. Nee, P. C. Hayes, B. M. Frier, L. A. Van Look, G. I. Johnston, R. M. Reynolds, et al. 2011. Prevalence of and risk factors for hepatic steatosis and nonalcoholic Fatty liver disease in people with type 2 diabetes: the Edinburgh Type 2 Diabetes Study. *Diabetes Care.* **34:** 1139–1144.
3. Hummasti, S., and G. S. Hotamisligil. 2010. Endoplasmic reticulum stress and inflammation in obesity and diabetes. *Circ. Res.* **107:** 579–591.
4. Brown, M. S., and J. L. Goldstein. 2008. Selective versus total insulin resistance: a pathogenic paradox. *Cell Metab.* **7:** 95–96.
5. Kido, Y., J. Nakae, and D. Accili. 2001. Clinical review 125: the insulin receptor and its cellular targets. *J. Clin. Endocrinol. Metab.* **86:** 972–979.
6. Li, S., M. S. Brown, and J. L. Goldstein. 2010. Bifurcation of insulin signaling pathway in rat liver: mTORC1 required for stimulation of lipogenesis, but not inhibition of gluconeogenesis. *Proc. Natl. Acad. Sci. USA.* **107:** 3441–3446.
7. Yecies, J. L., H. H. Zhang, S. Menon, S. Liu, D. Yecies, A. I. Lipovsky, C. Gorgun, D. J. Kwiatkowski, G. S. Hotamisligil, C. H. Lee, et al. 2011. Akt stimulates hepatic SREBP1c and lipogenesis through parallel mTORC1-dependent and independent pathways. *Cell Metab.* **14:** 21–32.
8. Assini, J. M., E. E. Mulvihill, B. G. Sutherland, D. E. Telford, C. G. Sawyez, S. L. Felder, S. Chhoker, J. Y. Edwards, R. Gros, and M. W. Huff. 2013. Naringenin prevents cholesterol-induced systemic inflammation, metabolic dysregulation, and atherosclerosis in *Ldlr*−/− mice. *J. Lipid Res.* **54:** 711–724.
9. Mulvihill, E. E., E. M. Allister, B. G. Sutherland, D. E. Telford, C. G. Sawyez, J. Y. Edwards, J. M. Markle, R. A. Hegele, and M. W. Huff. 2009. Naringenin prevents dyslipidemia, apolipoprotein B overproduction, and hyperinsulinemia in LDL receptor-null mice with diet-induced insulin resistance. *Diabetes.* **58:** 2198–2210.
10. Mulvihill, E. E., J. M. Assini, J. K. Lee, E. M. Allister, B. G. Sutherland, J. B. Koppes, C. G. Sawyez, J. Y. Edwards, D. E. Telford, A. Charbonneau, et al. 2011. Nobiletin attenuates VLDL overproduction, dyslipidemia, and atherosclerosis in mice with diet-induced insulin resistance. *Diabetes.* **60:** 1446–1457.
11. Dzamko, N. L., and G. R. Steinberg. 2009. AMPK-dependent hormonal regulation of whole-body energy metabolism. *Acta Physiol. (Oxf.).* **196:** 115–127.
12. Fullerton, M. D., G. R. Steinberg, and J. D. Schertzer. 2013. Immunometabolism of AMPK in insulin resistance and atherosclerosis. *Mol. Cell. Endocrinol.* **366:** 224–234.
13. Kemp, B. E., D. Stapleton, D. J. Campbell, Z. P. Chen, S. Murthy, M. Walter, A. Gupta, J. J. Adams, F. Katsis, B. van Denderen, et al. 2003. AMP-activated protein kinase, super metabolic regulator. *Biochem. Soc. Trans.* **31:** 162–168.
14. Steinberg, G. R., and B. E. Kemp. 2009. AMPK in health and disease. *Physiol. Rev.* **89:** 1025–1078.
15. Saggerson, D. 2008. Malonyl-CoA, a key signaling molecule in mammalian cells. *Annu. Rev. Nutr.* **28:** 253–272.
16. Evans, R. M., G. D. Barish, and Y. X. Wang. 2004. PPARs and the complex journey to obesity. *Nat. Med.* **10:** 355–361.
17. Bojic, L. A., and M. W. Huff. 2013. Peroxisome proliferator-activated receptor delta: a multifaceted metabolic player. *Curr. Opin. Lipidol.* **24:** 171–177.
18. Reilly, S. M., and C. H. Lee. 2008. PPAR delta as a therapeutic target in metabolic disease. *FEBS Lett.* **582:** 26–31.
19. Lee, C. H., P. Olson, A. Hevener, I. Mehl, L. W. Chong, J. M. Olefsky, F. J. Gonzalez, J. Ham, H. Kang, J. M. Peters, et al. 2006. PPARdelta regulates glucose metabolism and insulin sensitivity. *Proc. Natl. Acad. Sci. USA.* **103:** 3444–3449.
20. Tanaka, T., J. Yamamoto, S. Iwasaki, H. Asaba, H. Hamura, Y. Ikeda, M. Watanabe, K. Magoori, R. X. Ioka, K. Tachibana, et al. 2003. Activation of peroxisome proliferator-activated receptor delta induces fatty acid beta-oxidation in skeletal muscle and attenuates metabolic syndrome. *Proc. Natl. Acad. Sci. USA.* **100:** 15924–15929.
21. Wang, Y. X., C. H. Lee, S. Tiep, R. T. Yu, J. Ham, H. Kang, and R. M. Evans. 2003. Peroxisome-proliferator-activated receptor delta activates fat metabolism to prevent obesity. *Cell.* **113:** 159–170.
22. Nagasawa, T., Y. Inada, S. Nakano, T. Tamura, T. Takahashi, K. Maruyama, Y. Yamazaki, J. Kuroda, and N. Shibata. 2006. Effects of bezafibrate, PPAR pan-agonist, and GW501516, PPARdelta agonist, on development of steatohepatitis in mice fed a methionine- and choline-deficient diet. *Eur. J. Pharmacol.* **536:** 182–191.
23. Qin, X., X. Xie, Y. Fan, J. Tian, Y. Guan, X. Wang, Y. Zhu, and N. Wang. 2008. Peroxisome proliferator-activated receptor-delta induces insulin-induced gene-1 and suppresses hepatic lipogenesis in obese diabetic mice. *Hepatology.* **48:** 432–441.
24. Barroso, E., R. Rodriguez-Calvo, L. Serrano-Marco, A. M. Astudillo, J. Balsinde, X. Palomer, and M. Vazquez-Carrera. 2011. The PPARbeta/delta activator GW501516 prevents the down-regulation of AMPK caused by a high-fat diet in liver and amplifies the PGC-1alpha-lipin 1-PPARalpha pathway leading to increased fatty acid oxidation. *Endocrinology.* **152:** 1848–1859.
25. Liu, S., B. Hatano, M. Zhao, C. C. Yen, K. Kang, S. M. Reilly, M. R. Gangl, C. Gorgun, J. A. Balschi, J. M. Ntambi, et al. 2011. Role of peroxisome proliferator-activated receptor δ/β in hepatic metabolic regulation. *J. Biol. Chem.* **286:** 1237–1247.
26. Krämer, D. K., L. Al-Khalili, B. Guigas, Y. Leng, P. M. Garcia-Roves, and A. Krook. 2007. Role of AMP kinase and PPARdelta in the regulation of lipid and glucose metabolism in human skeletal muscle. *J. Biol. Chem.* **282:** 19313–19320.
27. Krämer, D. K., L. Al-Khalili, S. Perrini, J. Skogsberg, P. Wretenberg, K. Kannisto, H. Wallberg-Henriksson, E. Ehrenborg, J. R. Zierath, and A. Krook. 2005. Direct activation of glucose transport in primary human myotubes after activation of peroxisome proliferator-activated receptor delta. *Diabetes.* **54:** 1157–1163.
28. Barish, G. D., A. R. Atkins, M. Downes, P. Olson, L. W. Chong, M. Nelson, Y. Zou, H. Hwang, H. Kang, L. Curtiss, et al. 2008. PPARdelta regulates multiple proinflammatory pathways to suppress atherosclerosis. *Proc. Natl. Acad. Sci. USA.* **105:** 4271–4276.
29. Narkar, V. A., M. Downes, R. T. Yu, E. Embler, Y. X. Wang, E. Banayo, M. M. Mihaylova, M. C. Nelson, Y. Zou, H. Juguilon, et al. 2008. AMPK and PPARdelta agonists are exercise mimetics. *Cell.* **134:** 405–415.
30. Oliver, W. R., Jr., J. L. Shenk, M. R. Snaith, C. S. Russell, K. D. Plunket, N. L. Bodkin, M. C. Lewis, D. A. Winegar, M. L. Sznaidman, M. H. Lambert, et al. 2001. A selective peroxisome proliferator-activated receptor delta agonist promotes reverse cholesterol transport. *Proc. Natl. Acad. Sci. USA.* **98:** 5306–5311.
31. Lu, M., M. Wan, K. F. Leavens, Q. Chu, B. R. Monks, S. Fernandez, R. S. Ahima, K. Ueki, C. R. Kahn, and M. J. Birnbaum. 2012. Insulin regulates liver metabolism in vivo in the absence of hepatic Akt and Foxo1. *Nat. Med.* **18:** 388–395.
32. Mulvihill, E. E., J. M. Assini, B. G. Sutherland, A. S. DiMattia, M. Khami, J. B. Koppes, C. G. Sawyez, S. C. Whitman, and M. W. Huff. 2010. Naringenin decreases progression of atherosclerosis by improving dyslipidemia in high-fat-fed low-density lipoprotein receptor-null mice. *Arterioscler. Thromb. Vasc. Biol.* **30:** 742–748.
33. Cool, B., B. Zinker, W. Chiou, L. Kifle, N. Cao, M. Perham, R. Dickinson, A. Adler, G. Gagne, R. Iyengar, et al. 2006. Identification and characterization of a small molecule AMPK activator that treats key components of type 2 diabetes and the metabolic syndrome. *Cell Metab.* **3:** 403–416.
34. Hawley, S. A., M. D. Fullerton, F. A. Ross, J. D. Schertzer, C. Chevtzoff, K. J. Walker, M. W. Peggie, D. Zibrova, K. A. Green, K. J. Mustard, et al. 2012. The ancient drug salicylate directly activates AMP-activated protein kinase. *Science.* **336:** 918–922.

35. Dzamko, N., B. J. van Denderen, A. L. Hevener, S. B. Jorgensen, J. Honeyman, S. Galic, Z. P. Chen, M. J. Watt, D. J. Campbell, G. R. Steinberg, et al. 2010. AMPK beta1 deletion reduces appetite, preventing obesity and hepatic insulin resistance. *J. Biol. Chem.* **285:** 115–122.
36. Scott, J. W., B. J. van Denderen, S. B. Jorgensen, J. E. Honeyman, G. R. Steinberg, J. S. Oakhill, T. J. Iseli, A. Koay, P. R. Gooley, D. Stapleton, et al. 2008. Thienopyridone drugs are selective activators of AMP-activated protein kinase beta1-containing complexes. *Chem. Biol.* **15:** 1220–1230.
37. Steinberg, G. R., B. J. Michell, B. J. van Denderen, M. J. Watt, A. L. Carey, B. C. Fam, S. Andrikopoulos, J. Proietto, C. Z. Gorgun, D. Carling, et al. 2006. Tumor necrosis factor alpha-induced skeletal muscle insulin resistance involves suppression of AMP-kinase signaling. *Cell Metab.* **4:** 465–474.
38. Watt, M. J., N. Dzamko, W. G. Thomas, S. Rose-John, M. Ernst, D. Carling, B. E. Kemp, M. A. Febbraio, and G. R. Steinberg. 2006. CNTF reverses obesity-induced insulin resistance by activating skeletal muscle AMPK. *Nat. Med.* **12:** 541–548.
39. Chen, M. B., A. J. McAinch, S. L. Macaulay, L. A. Castelli, P.E. O'Brien, J. B. Dixon, D. Cameron-Smith, B. E. Kemp, and G. R. Steinberg. 2005. Impaired activation of AMP-kinase and fatty acid oxidation by globular adiponectin in cultured human skeletal muscle of obese type 2 diabetics. *J. Clin. Endocrinol. Metab.* **90:** 3665–3672.
40. Folch, J., M. Lees, and G. H. Sloane Stanley. 1957. A simple method for the isolation and purification of total lipides from animal tissues. *J. Biol. Chem.* **226:** 497–509.
41. Beyea, M. M., C. L. Heslop, C. G. Sawyez, J. Y. Edwards, J. G. Markle, R. A. Hegele, and M. W. Huff. 2007. Selective up-regulation of LXR-regulated genes ABCA1, ABCG1, and APOE in macrophages through increased endogenous synthesis of 24(S),25-epoxycholesterol. *J. Biol. Chem.* **282:** 5207–5216.
42. Rowe, A. H., C. A. Argmann, J. Y. Edwards, C. G. Sawyez, O. H. Morand, R. A. Hegele, and M. W. Huff. 2003. Enhanced synthesis of the oxysterol 24(S),25-epoxycholesterol in macrophages by inhibitors of 2,3-oxidosqualene:lanosterol cyclase: a novel mechanism for the attenuation of foam cell formation. *Circ. Res.* **93:** 717–725.
43. Fullerton, M. D., S. Galic, K. Marcinko, S. Sikkema, T. Pulinilkunnil, Z. P. Chen, H. M. O'Neill, R. J. Ford, R. Palanivel, M. O'Brien, et al. 2013. Single phosphorylation sites in Acc1 and Acc2 regulate lipid homeostasis and the insulin-sensitizing effects of metformin. *Nat. Med.* **19:** 1649–1654.
44. Beyea, M. M., S. Reaume, C. G. Sawyez, J. Y. Edwards, C. O'Neil, R. A. Hegele, J. G. Pickering, and M. W. Huff. 2012. The oxysterol 24(s),25-epoxycholesterol attenuates human smooth muscle-derived foam cell formation via reduced low-density lipoprotein uptake and enhanced cholesterol efflux. *J Am Heart Assoc.* **1:** e000810.
45. Bojic, L. A., A. C. Burke, S. S. Chhoker, D. E. Telford, B. G. Sutherland, J. Y. Edwards, C. G. Sawyez, R. G. Tirona, H. Yin, J. G. Pickering, et al. 2014. Peroxisome proliferator-activated receptor delta agonist GW1516 attenuates diet-induced aortic inflammation, insulin resistance, and atherosclerosis in low-density lipoprotein receptor knockout mice. *Arterioscler. Thromb. Vasc. Biol.* **34:** 52–60.
46. Chawla, A., C. H. Lee, Y. Barak, W. He, J. Rosenfeld, D. Liao, J. Han, H. Kang, and R. M. Evans. 2003. PPARdelta is a very low-density lipoprotein sensor in macrophages. *Proc. Natl. Acad. Sci. USA.* **100:** 1268–1273.
47. Bojic, L. A., C. G. Sawyez, D. E. Telford, J. Y. Edwards, R. A. Hegele, and M. W. Huff. 2012. Activation of peroxisome proliferator-activated receptor delta inhibits human macrophage foam cell formation and the inflammatory response induced by very low-density lipoprotein. *Arterioscler. Thromb. Vasc. Biol.* **32:** 2919–2928.
48. Van Beek, M., K. I. Oravecz-Wilson, P. C. Delekta, S. Gu, X. Li, X. Jin, I. J. Apel, K. S. Konkle, Y. Feng, D. H. Teitelbaum, et al. 2012. Bcl10 links saturated fat overnutrition with hepatocellular NF-kB activation and insulin resistance. *Cell Reports.* **1:** 444–452.
49. Kaplowitz, N., T. A. Than, M. Shinohara, and C. Ji. 2007. Endoplasmic reticulum stress and liver injury. *Semin. Liver Dis.* **27:** 367–377.
50. Peterson, T. R., S. S. Sengupta, T. E. Harris, A. E. Carmack, S. A. Kang, E. Balderas, D. A. Guertin, K. L. Madden, A. E. Carpenter, B. N. Finck, et al. 2011. mTOR complex 1 regulates lipin 1 localization to control the SREBP pathway. *Cell.* **146:** 408–420.
51. Gregor, M. F., and G. S. Hotamisligil. 2011. Inflammatory mechanisms in obesity. *Annu. Rev. Immunol.* **29:** 415–445.
52. Liang, C. P., S. Han, T. Senokuchi, and A. R. Tall. 2007. The macrophage at the crossroads of insulin resistance and atherosclerosis. *Circ. Res.* **100:** 1546–1555.
53. Tabas, I., A. Tall, and D. Accili. 2010. The impact of macrophage insulin resistance on advanced atherosclerotic plaque progression. *Circ. Res.* **106:** 58–67.
54. Odegaard, J. I., R. R. Ricardo-Gonzalez, A. Red Eagle, D. Vats, C. R. Morel, M. H. Goforth, V. Subramanian, L. Mukundan, A. W. Ferrante, and A. Chawla. 2008. Alternative M2 activation of Kupffer cells by PPARdelta ameliorates obesity-induced insulin resistance. *Cell Metab.* **7:** 496–507.